

ARM Data-Oriented Metrics and Diagnostics Package (ARM-Diags) for Climate Model Evaluation

C Tao
S Xie
X Zheng

C Zhang
M Zhang

October 2024



DISCLAIMER

This report was prepared as an account of work sponsored by the U.S. Government. Neither the United States nor any agency thereof, nor any of their employees, makes any warranty, express or implied, or assumes any legal liability or responsibility for the accuracy, completeness, or usefulness of any information, apparatus, product, or process disclosed, or represents that its use would not infringe privately owned rights. Reference herein to any specific commercial product, process, or service by trade name, trademark, manufacturer, or otherwise, does not necessarily constitute or imply its endorsement, recommendation, or favoring by the U.S. Government or any agency thereof. The views and opinions of authors expressed herein do not necessarily state or reflect those of the U.S. Government or any agency thereof.

ARM Data-Oriented Metrics and Diagnostics Package (ARM-Diags) for Climate Model Evaluation

C Tao, Lawrence Livermore National Laboratory (LLNL)
C Zhang, LLNL
S Xie, LLNL
M Zhang, Stony Brook University
X Zheng, Argonne National Laboratory

October 2024

How to cite this document:

Tao, C, C Zhang, S Xie, M Zhang, and X Zheng. 2024. ARM Data-Oriented Metrics and Diagnostics Package (ARM-Diags) for Climate Model Evaluation. U.S. Department of Energy, Atmospheric Radiation Measurement user facility, Richland, Washington. DOE/SC-ARM-TR-202.

Work supported by the U.S. Department of Energy,
Office of Science, Office of Biological and Environmental Research

Acronyms and Abbreviations

| | |
|------------|--|
| ACSM | aerosol chemical speciation monitor |
| AMIP | Atmospheric Model Intercomparison Project |
| AOD | aerosol optical depth |
| ARM | Atmospheric Radiation Measurement |
| ARMBE | ARM Best Estimate Data Products |
| ARM-Diags | ARM Data-Oriented Metrics and Diagnostics Package |
| BOM | Bureau of Meteorology, Australia |
| CCN | cloud condensation nuclei |
| CDAT | Project Critical Decision Assessment Tool |
| CF | Central Facility |
| CMIP | Coupled Model Intercomparison Project |
| CPC | condensation particle counter |
| DOE | U.S. Department of Energy |
| DOI | Digital Object Identifier |
| EF | evaporative fraction |
| ENA | Eastern North Atlantic |
| GCM | global climate model |
| HTML | Hypertext Markup Language |
| L-A | land-atmosphere |
| LCL | lifting condensation level |
| LLNL | Lawrence Livermore National Laboratory |
| MAO | Manacapuru, Brazil |
| MFRSR | multifilter rotating shadowband radiometer |
| MFRSRCLDOD | Cloud Optical Properties from the Multifilter Rotating Shadowband Radiometer Value-Added Product |
| NSA | North Slope of Alaska |
| PBL | planetary boundary layer |
| PBLH | planetary boundary layer height |
| PDF | probability density function |
| SGP | Southern Great Plains |
| SWATS | soil water and temperature systems |
| TWP | Tropical Western Pacific |
| VAP | value-added product |
| VARANAL | Constrained Variational Analysis Value-Added Product |

Contents

| | |
|--|-----|
| Acronyms and Abbreviations | iii |
| 1.0 Introduction | 1 |
| 2.0 Overview of Metrics in the ARM-Diags | 1 |
| 3.0 Description of Data in the ARM-Diags | 3 |
| 3.1 Observational Data Sets | 3 |
| 3.2 CMIP Simulations | 4 |
| 3.3 Data Limitation and Uncertainty | 6 |
| 4.0 User’s Guide | 6 |
| 4.1 Package Workflow | 6 |
| 4.2 Obtain the ARM-Diags | 7 |
| 4.3 Set Up a Test Case | 8 |
| 4.4 Diagnostics Examples | 9 |
| 5.0 References | 11 |

Figures

| | |
|--|----|
| 1 Workflow of the diagnostics package. | 6 |
| 2 Main html page generated to host the diagnostics results. | 8 |
| 3 (left) Summer (June-July-August) mean diurnal cycle of precipitation (dot) and the first Fourier component (line) from the ARM observations (black), test model (red), and CMIP6 AMIP runs (gray lines for individual CMIP6 models and blue line for multimodel mean). (right) Harmonic dial plots of summer precipitation amplitude (mm/day) and phase of the first Fourier component at the ARM SGP site. | 9 |
| 4 Probability density plots for aerosol number concentration (x-axis) versus CCN number concentration (y-axis) at 0.2% supersaturation level for (a) ARM observations and (b) test model at the ARM ENA site. | 10 |
| 5 Top: Scatter plots of (left) surface sensible heat flux, (middle) surface latent heat flux, and (right) EF versus LCL at the ARM SGP site during the summer (June-July-August). Bottom: Same as the top but from the model simulations. | 10 |

Tables

| | |
|--|---|
| 1 Metrics and diagnostics available in the ARM-Diags version 4.0. | 2 |
| 2 Observed quantities included in the evaluation package for SGP | 4 |
| 3 Observed quantities included in the evaluation package for other ARM sites. | 4 |
| 4 CMIP5 and CMIP6 models included in the evaluation package. | 4 |

1.0 Introduction

A Python-based metrics and diagnostics package was developed by the U.S. Department of Energy (DOE) Atmospheric Radiation Measurement (ARM) user facility Infrastructure Team at Lawrence Livermore National Laboratory (LLNL) to facilitate the use of long-term, high-frequency measurements from the ARM facility on model evaluation. This metrics and diagnostics package, ARM-Diags, computes climatological means of targeted climate model simulation and generates tables and plots using a fully automated framework (Zhang et al. 2020). Users can then compare their model simulations directly with the ARM observations. The Coupled Model Intercomparison Project (CMIP) model data sets are also included in the package to enable model intercomparison (Zhang et al. 2018, Zheng et al. 2023). The ensemble means of CMIP models can serve as a reference for individual models as well.

Basic performance metrics are computed to measure the accuracy of mean state and variability of climate models. The evaluated physical quantities include cloud fraction, temperature, relative humidity, cloud liquid water path, total column water vapor, precipitation, sensible and latent heat fluxes, radiative fluxes, aerosol properties, soil moistures, planetary boundary layer, etc. ARM-Diags also includes other variables that describe the coupling of the atmosphere with processes associated with land, aerosols, clouds, precipitation, and process-oriented diagnostics.

The ARM-Diags is currently built upon standard Python libraries and additional Python packages developed by DOE (Project Critical Decision Assessment Tool [CDAT]). It is available to the public and can serve as an easy entry point for climate modelers to quickly compare their models with ARM observations and the supplemented CMIP data sets.

In this report, we first provide an overview of the metrics included in the ARM-Diags in section 2. The input data sets, which constitute the core content of the metrics and diagnostics package, are summarized in section 3. Section 4 documents the current workflow of the ARM-Diags and provides step-by-step instructions for users' reference.

2.0 Overview of Metrics in the ARM-Diags

The standard metrics and diagnostics included in the ARM-Diags version 2.0 (v2) are summarized in Zhang et al. (2020), which covers the basic diagnostics on various climate variabilities (e.g., annual, seasonal, and diurnal cycles) as well as metrics that enable process-level studies. Particularly, the convection onset metrics quantifying robust relationships between precipitation, column water vapor, and temperature (Schiro et al. 2016) were added to ARM-Diags as the first set of process-oriented diagnostics. This convection onset metrics help evaluate the model performance on deep convection with the ARM observations.

The development of the ARM-Diags v3 focuses on the metrics and diagnostics for the aerosol-cloud interactions. Statistical metrics including the annual cycle of aerosol optical depth (AOD), aerosol and cloud condensation nuclei (CCN) number concentration, and aerosol chemicals (organic, sulfate, nitrate, etc.) were added. Moreover, another process-oriented diagnostic, the aerosol-CCN activation metrics, were developed to quantify the statistical relationship between the aerosol and CCN number

concentration at certain supersaturation levels (Zheng et al. 2020). With these metrics, users can quickly assess the aerosol activation parameterization in their models, which serves as a solid entry point for the further assessment of the simulated aerosol indirect effects.

The ARM-Diags v4 has been extended to include the metrics and diagnostics on the land-atmosphere (L-A) coupling. Specifically, basic statistical metrics on the diurnal cycles of surface sensible and latent heat fluxes, planetary boundary layer (PBL) and lifting condensation level (LCL) currently available at the ARM Southern Great Plains (SGP) site have been added. The two-legged metrics, which can be used to estimate the coupling strength between the land and the atmosphere based on a land leg and an atmospheric leg (Dirmeyer et al. 2014, Santanello et al. 2018), were also added. The inclusion of metrics on the L-A coupling enables quick evaluation of model-simulated L-A coupling processes against ARM ground-based observations.

A full list of the metrics and diagnostics are as follows, with detailed information summarized in Table 1:

- a set of basic metrics tables: mean, mean bias, correlation, and root-mean-square error based on the annual cycle of each variable.
- line plots and Taylor diagrams (Taylor 2001) for the annual cycle of each variable.
- contour and vertical profiles of the annual cycle and the diurnal cycle of cloud fraction.
- line and harmonic dial plots (Covey et al. 2016) of the diurnal cycle of precipitation.
- probability density function (PDF) plots of precipitation (Pendergrass and Hartmann 2014).
- line plots of the diurnal cycle for quantities relevant to the L-A coupling (e.g., surface sensible and latent heat fluxes, PBL, LCL, etc.).
- convection onset metrics showing the statistical relationship between precipitation rate and column water vapor (Schiro et al. 2016).
- aerosol-CCN activation metrics describing the percentage distribution of how many aerosols can be activated as CCN under different supersaturation levels (Zheng et al. 2020).
- two-legged metrics evaluating the strength of L-A coupling by partitioning the impact of the land states on surface fluxes (the land leg) and from the impact of surface fluxes on the atmospheric states (the atmospheric leg) (Dirmeyer et al. 2014, Santanello et al. 2018).

Table 1. Metrics and diagnostics available in the ARM-Diags version 4.0.

| Basic diagnostics sets | Input variables | Available sites |
|--|---|--|
| Statistical summary of mean state (annual cycle, Taylor diagram) | <p><i>Aerosol properties:</i> CCN number concentration at 0.2% and 0.5% supersaturations,* aerosol number concentration,* aerosol chemical component mass concentrations.*</p> <p><i>Column properties:</i> cloud fraction, cloud optical depth,* column precipitable water vapor, AOD.</p> <p><i>Surface properties:</i> sensible and latent heat fluxes, relative humidity, temperature, precipitation,</p> | SGP C1; NSA C1; ENA C1; MAO M1; TWP C1, C2, C3 |

| Basic diagnostics sets | Input variables | Available sites |
|------------------------------------|--|--|
| | downwelling shortwave and longwave fluxes, upwelling shortwave and longwave fluxes, soil moisture.** | |
| Vertical variabilities | Cloud fraction | SGP C1; NSA C1; ENA C1; MAO M1; TWP C1, C2, C3 |
| Diurnal and seasonal variabilities | Precipitation | SGP C1; ENA C1; MAO M1; TWP C1, C2, C3 |
| | Sensible and latent heat fluxes, relative humidity, temperature, PBL, LCL | SGP C1 |
| Process-oriented diagnostics sets | Input variables | Available sites |
| Convection onset | Column precipitable water vapor and surface precipitation (hourly) | SGP C1; ENA C1; TWP C1, C2, C3; MAO M1 |
| Aerosol-CCN activation | Aerosol and CCN number concentrations (5-min) | SGP C1; ENA C1 |
| Two-legged metrics | Sensible and latent heat fluxes, LCL and soil moisture** (daily) | SGP C1 |

*Variables available at SGP C1 and ENA C1 only.

** Variables available at SGP C1 only.

3.0 Description of Data in the ARM-Diags

3.1 Observational Data Sets

The observational data sets used to assess model performance are primarily from the ARM Best Estimate Data Products (ARMBE; Xie et al. 2010) as well as other ARM value-added products (VAPs) available for all the ARM observatories and some ARM mobile facilities. These data often rely on measurements at the ARM Central Facility (CF) locations (i.e., single-point measurements). At the ARM SGP site, particularly, the long-term continuous forcing data derived based on a constrained variational analysis (VARANAL; Zhang and Lin 1997, Zhang et al. 2001, Xie et al. 2004, Tang et al. 2019) is applied to improve model-observation comparison. Different from the single-point observations at the ARM CF, the VARANAL data set represents an average over a domain with size comparable to a grid box in a global climate model (GCM). Aerosol properties are collected from the condensation particle counter (CPC), cloud condensation nuclei particle counter (CCN), aerosol chemical speciation monitor (ACSM), and multifilter rotating shadowband radiometer (MFRSR) at the SGP and ENA sites, which are carefully processed by applying several quality control procedures. The diurnal variability of PBL height for the L-A coupling metrics is from Su and Li (2023), who developed a new lidar-based algorithm for retrieving PBL height under cloudy conditions and provided quality-controlled, long-term, continuous retrievals of the PBL height at SGP during the daytime (Su et al. 2020, 2022). Detailed information on the ARM data applied in the ARM-Diags v4 is listed in Tables 2 and 3.

Table 2. Observed quantities included in the evaluation package for SGP.

| Quantities | Data sources | Time range | Time reso. | Spatial info. |
|--|---|------------|-------------------|------------------------|
| Surface temperature/humidity | VARANAL | 2004-2015 | mon, day, hr | domain averaged |
| Temperature/humidity profile/wind speed/large-scale tendencies | | | | |
| Surface precipitation | | | | |
| Precipitable water | | | | |
| Surface all-sky radiative fluxes | | | | |
| Surface latent/sensible heat fluxes | | | | |
| Aerosol optical depth 550 nm | MFRSRAOD1MICH | 2004-2015 | mon | SGP C1 and E13 average |
| Soil moisture content (10 cm) | SWATS | 2004-2015 | mon, day | domain averaged |
| Cloud fraction | ARMBE | 2004-2015 | mon, day, hr | SGP C1 |
| Cloud optical depth | MFRSRCLDOD1MIN | 2004-2015 | mon | SGP C1 |
| Cloud condensation nuclei | CCN1COL | 2011-2016 | mon, 5-min | SGP C1 |
| Aerosol number concentration | CPC | 2011-2016 | mon, 5-min | SGP C1 |
| Aerosol chemical component | ACSM | 2011-2016 | mon, 5-min | SGP C1 |
| Planetary boundary layer | PBLH over SGP from 1998 to 2023 | 2004-2015 | hr (daytime only) | SGP C1 |

Table 3. Observed quantities included in the evaluation package for other ARM sites.

| Quantities | Data sources | Spatial info. (Time range) | Time reso. |
|-------------------------------------|----------------|--|--------------|
| Cloud fraction | ARMBE | NSA C1 (2001-2016); ENA C1 (2016-2019); TWP C1 (1998-2009); TWP C2 (1999-2010); TWP C3 (2003-2010); MAO M1 (2014-2015); | mon, day, hr |
| Surface temperature/humidity | | | |
| Surface precipitation | | | |
| Precipitable water | | | |
| Surface all-sky radiative fluxes | | | |
| Surface latent/sensible heat fluxes | | | |
| Aerosol optical depth 550 nm | MFRSRAOD1MICH | Same as above | mon |
| Cloud optical depth | MFRSRCLDOD1MIN | Same as above | mon |
| Cloud condensation nuclei | CCN1COL | ENA C1 (2016-2019) | mon, 5-min |
| Aerosol number concentration | CPC | ENA C1 (2016-2019) | mon, 5-min |
| Aerosol chemical component | ACSM | ENA C1 (2016-2019) | mon, 5-min |

3.2 CMIP Simulations

Simulations of 23 models contributing to Phase 6 of the Coupled Model Intercomparison Project (CMIP6; Eyring et al. 2016) are added in the ARM-Diags v4 (Table 4), which allows modelers to compare a new, candidate version of their model to existing CMIP models. Here, we used the CMIP6 atmospheric only (AMIP) experiments from 1979 to 2008. Results from CMIP5 (Taylor et al. 2012) AMIP experiments are included as well for users' reference. The nearest model grid points to the ARM sites are selected.

Table 4. CMIP5 and CMIP6 models included in the evaluation package.

| Modeling groups | CMIP5 model name | CMIP6 model name |
|--|-------------------------------|------------------|
| Commonwealth Scientific and Industrial Research Organization; Bureau of Meteorology (BOM), Australia | ACCESS-1-0 ACCESS-3-0 | ACCESS-ESM1-5 |
| Beijing Climate Center, China Meteorological Administration, China | BCC-CSM-1-1 BCC-CSM-1-1(m) | BCC-CSM2-MR |

| Modeling groups | CMIP5 model name | CMIP6 model name |
|--|--|---------------------------------|
| College of Global Change and Earth System Science, Beijing Normal University, China | BNU-ESM | |
| Chinese Academy of Meteorological Sciences, China | | CAMS-CSM1-0 |
| Canadian Centre for Climate Modelling and Analysis, Canada | CanAM4 | CanESM5 |
| National Center for Atmospheric Research, USA | CCSM4 | |
| Community Earth System Model Contributors | CESM1-CAM5 | CESM2 CESM2-WACCM |
| Centro Euro-Mediterranean Centre on Climate Change, Italy | CMCC-CM | CMCC-CM2-SR5 |
| Centre National de Recherches Météorologiques, France | CNRM-CM5 | CNRM-CM6-1-HR |
| Commonwealth Scientific and Industrial Research Organization; Queensland Climate Change Centre of Excellence, Australia | CSIRO-Mk3-6-0 | |
| Energy Exascale Earth System Model Contributors | | E3SM-1-0 |
| European Centre for Medium-Range Weather Forecasts | EC-Earth | EC-Earth3-AerChem |
| Institute of Atmospheric Physics, Chinese Academy of Sciences; Center for Earth System Science, Tsinghua University, China | FGOALS-g2 FGOALS-s2 | FGOALS-f3-L |
| NOAA Geophysical Fluid Dynamics Laboratory, USA | GFDL-HIRAM-C360 GFDL-HIRAM-C180 | GFDL-CM4 |
| NASA Goddard Institute for Space Studies, USA | GISS-E2-R | GISS-E2-1-G |
| Met Office Hadley Centre, UK | HadGEM2-A | HadGEM3-GC31-LL |
| Institute Pierre-Simon Laplace, France | IPSL-CM5A-LR IPSL-CM5B-LR IPSL-CM5A-MR | IPSL-CM6A-LR |
| Centre for Climate Change Research, Indian Institute of Tropical Meteorology, India | | IITM-ESM |
| Institute for Numerical Mathematics, Russia | INM-CM4 | INM-CM5-0 |
| National Institute of Meteorological Sciences; Korea Meteorological Administration, Korea | | KACE-1-0-G |
| Atmosphere and Ocean Research Institute; National Institute for Environmental Studies; and Japan Agency for Marine-Earth Science and Technology, Japan | MIROC5 | MIROC6 |
| Max Planck Institute for Meteorology, Germany | MPI-ESM-LR MPI-ESM-MR | MPI-ESM1-2-HAM MPI-ESM1-2-HR |
| Meteorological Research Institute, Japan | MRI-AGCM-3-2 MRI-CGCM-3 | MRI-ESM-2-0 |
| Earth System Modeling Center, Nanjing University of Information Science and Technology, China | | NESM3 |
| Norwegian Climate Centre, Norway | NorESM1-M | NorESM2-LM |
| Research Center for Environmental Changes, Academia Sinica, Taiwan | | TaiESM1 |

*Note that a subset of models are used for quantities required in daily or sub-daily temporal resolutions.

3.3 Data Limitation and Uncertainty

The ARM data used in the package have been through stringent data quality control and represent the “best” estimate of the selected quantities. Fully addressing the data uncertainty is a challenging task and ARM is addressing this issue. We recommend users to read the references on the observational data products and contact principal investigators of each data product for additional data quality information.

4.0 User’s Guide

4.1 Package Workflow

Figure 1 shows the flowchart of creating the diagnostic results by applying the diagnostics tool. Section 4.2 provides instructions on how to obtain the package. The step-by-step procedure on setting up a working prototype is presented in section 4.3.

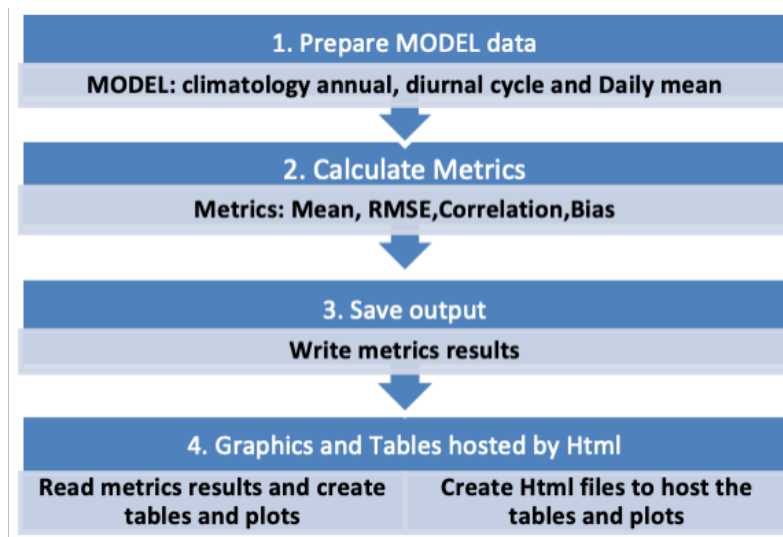


Figure 1. Workflow of the diagnostics package.

The project has the following structure:

```

|__arm_diags
| |___.DS_Store
| |___.init__.py
| |___.arm_driver.py
| |___.arm_parameter.py
| |___.arm_parser.py
| |___.basicparameter.py
| |___.diags_all_multisites_for_cmip5.json
| |___.diags_all_multisites_for_cmip6.json
| |___.examples
| | |___.diags_set1.json
| | |___.diags_set2.json
| | |___.diags_set3.json
  
```

```

| |__misc
| | |__ARM_DIAGS_logo.png
| | |__ARM_logo.png
| |__src
| | |__init__.py
| | |__aerosol_activation.py
| | |__annual_cycle.py
| | |__annual_cycle_aci.py
| | |__annual_cycle_zt.py
| | |__convection_onset_driver.py
| | |__convection_onset_statistics.py
| | |__create_htmls.py
| | |__diurnal_cycle.py
| | |__diurnal_cycle_LAcoupling.py
| | |__pdf_daily.py
| | |__seasonal_mean.py
| | |__taylor_diagram.py
| | |__twolegged_metric.py
| | |__utils.py
| | |__varid_dict.py
|__ARM_DIAGS_TechReport_v4.docx

```

4.2 Obtain the ARM-Diags

The ARM-Diags v4 with both basic statistical and process-oriented diagnostics sets is now available to the public. The main html page hosting the results is shown in Figure 2. The data files, including observation, and CMIP5 and CMIP6 model data, can be downloaded through the [ARM Data Center](#). The analytical codes to calculate and visualize the diagnostics results are placed via repository (arm-gcm-diagnostics) at <https://github.com/ARM-DOE/arm-gcm-diagnostics>.

For downloading data:

- Click www.arm.gov/data/data-sources/adcme-123
- Follow the **Browse Data** link on that page: it will lead to the area where the data files are placed. A short registration is required if you do not have an ARM account.
- The DOI for the citation of the data is 10.5439/1646838

For obtaining codes:

```
$ git clone https://github.com/ARM-DOE/arm-gcm-diagnostics/
```

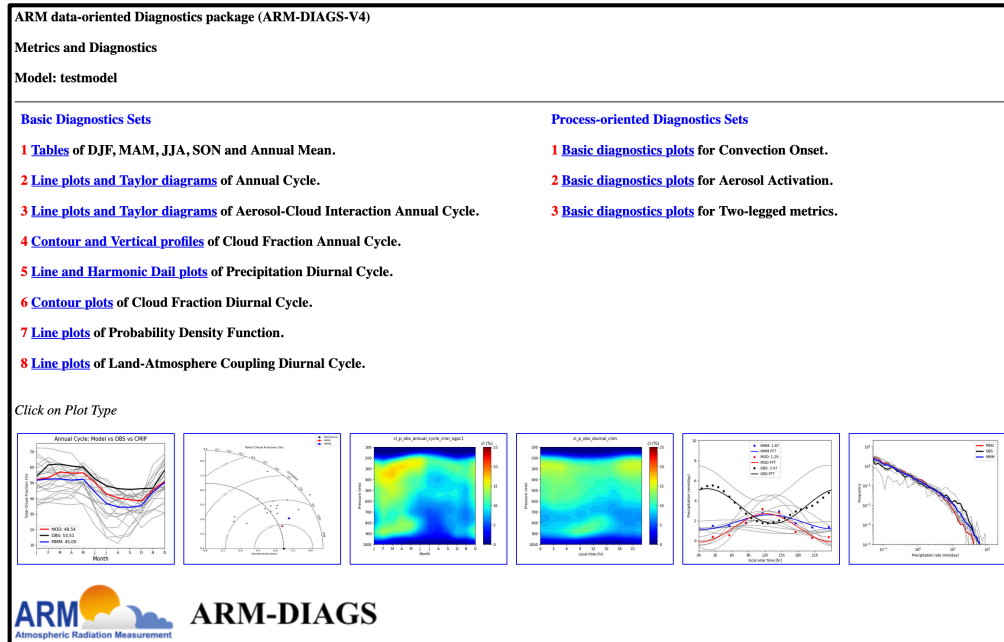


Figure 2. Main html page generated to host the diagnostics results.

4.3 Set Up a Test Case

The software environment is managed through conda. Either Anaconda or Miniconda needs to be installed for setting up the environment of the package.

1. To create a conda environment and then activate it:

```
$conda create -n arm_diags_env_py3 cdp cdtutil cdms2 libcdms matplotlib scipy python=3 -c conda-forge
```

```
$source activate arm_diags_env_py3
```

2. To install the package, cd <Your directory>/, type the following:

```
$python setup.py install
```

3. A working test case has been set up for users to run the package out of the box. In this case, all the observation, CMIP, and test data should be downloaded and placed under directories:

<Your directory>/arm_diags/observation

<Your directory>/arm_diags/cmip6

<Your directory>/arm_diags/testmodel, respectively.

4. To configure a basic parameter file: basicparameter.py and edit parameters such as input and output paths, model name (used to search the file), and case name (to create a new folder for the case).
5. To run the package, simply type in the terminal the following:

```
$ python arm_driver.py -p basicparameter.py
```

6. To view the diagnostics results:

For Mac OS:

```
$ open <User defined output directory>/html/ARM_diag.html
```

For Linux:

```
$ xdg-open <User defined output directory>/html/ARM_diag.html
```

For setting up customized runs and creating new cases, please refer to details at: <https://github.com/ARM-DOE/arm-gcm-diagnostics/>

4.4 Diagnostics Examples

Diurnal cycle of precipitation. Multiple aspects of the precipitation (total amount, frequency, intensity, and duration, etc.) can be effectively diagnosed through the diurnal cycle of precipitation, which is therefore considered a benchmark for climate models (Covey et al. 2016). With this metrics, users can quickly evaluate the convection parameterizations in their models. Figure 3 shows an example of the metrics on the diurnal cycle of precipitation at the ARM SGP site during summer. The observed nocturnal peak, associated with the eastward propagation of mesoscale convective systems, is missed by the model simulations and CMIP6 AMIP runs.

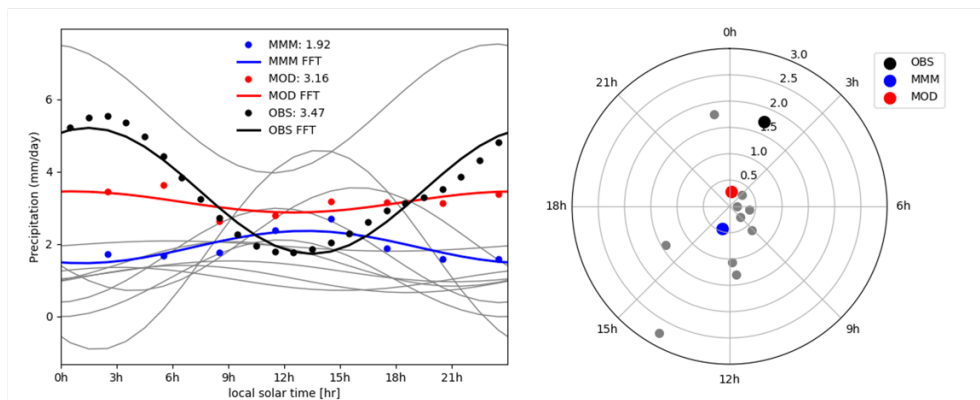


Figure 3. (left) Summer (June-July-August) mean diurnal cycle of precipitation (dot) and the first Fourier component (line) from the ARM observations (black), test model (red), and CMIP6 AMIP runs (gray lines for individual CMIP6 models and blue line for multimodel mean). (right) Harmonic dial plots of summer precipitation amplitude (mm/day) and phase of the first Fourier component at the ARM SGP site.

Aerosol-CCN activation metrics. Aerosol-CCN activation metrics allow users to quantify the statistical relationship between the aerosol and CCN number concentration (Zheng et al. 2023). An example of the aerosol-CCN activation metrics at ENA is shown in Figure 4. Compared to the ARM observations, the model tends to predict too many aerosols that cannot be activated to CCN at 0.2% supersaturation levels. This suggests that the model may overproduce the aerosol over such pristine oceanic regions.

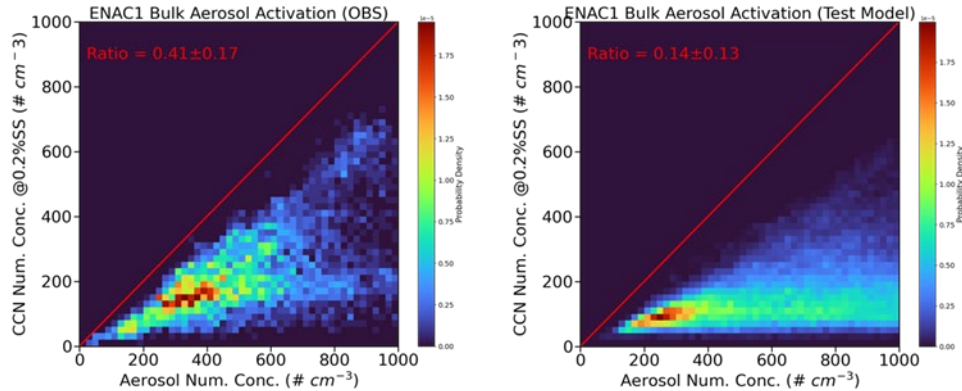


Figure 4. Probability density plots for aerosol number concentration (x-axis) versus CCN number concentration (y-axis) at 0.2% supersaturation level for (a) ARM observations and (b) test model at the ARM ENA site.

Two-legged metrics. Two-legged metrics evaluate the L-A coupling as a two-segment process: a terrestrial leg linking land states to surface fluxes and an atmospheric leg linking surface fluxes to atmosphere states (e.g., Dirmeyer et al. 2014, Santanello et al. 2018). For the terrestrial leg, we focus on the covariance relationships between soil moisture and surface turbulent fluxes. For the atmospheric leg, we emphasize the covariance relationships between surface turbulent fluxes and LCL, which is a good indicator for the potential of rain. Figure 5 shows an example of the atmospheric component for the two-legged metrics at the ARM SGP site during summer. Generally, there is a strong coupling between the evaporative fraction (EF) and LCL in both observations and model simulations, where the LCL tends to be lower with a larger EF. But the coupling strength is stronger in the model than that in the ARM observations.

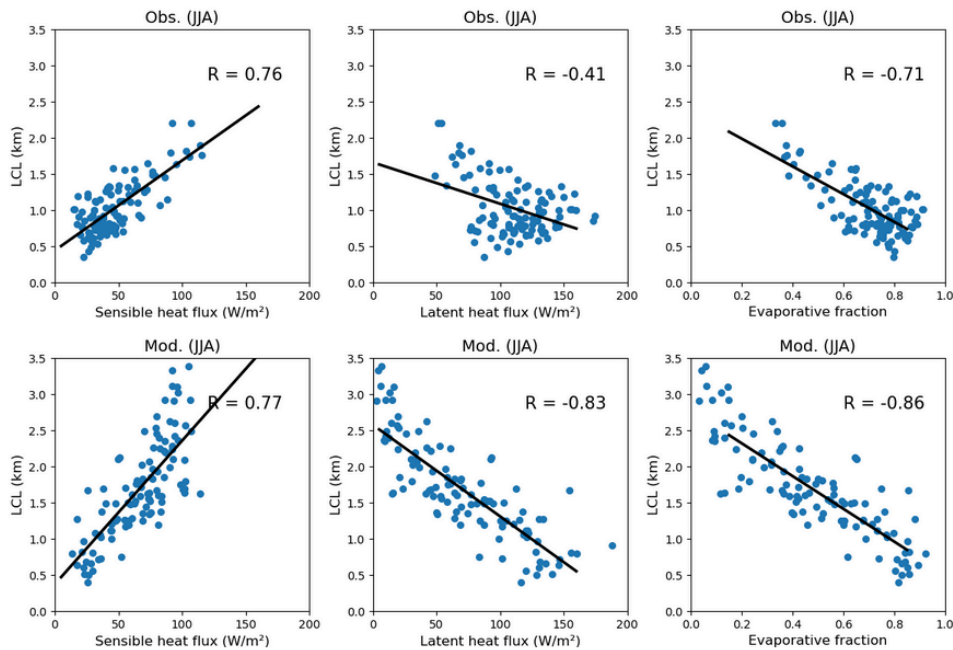


Figure 5. Top: Scatter plots of (left) surface sensible heat flux, (middle) surface latent heat flux, and (right) EF versus LCL at the ARM SGP site during the summer (June-July-August). Bottom: Same as the top but from the model simulations.

5.0 References

- Covey, C, PJ Gleckler, CM Doutriaux, DN Williams, A Dai, JT Fasullo, K Trenberth, and A Berg. 2016. “Metrics for the diurnal cycle of precipitation: Toward routine benchmarks for climate models.” *Journal of Climate* 29(12): 4461–4471, <https://doi.org/10.1175/JCLI-D-15-0664.1>
- Dirmeyer, PA, Z Wang, MJ Mbuh, and HE Norton. 2014. “Intensified land surface control on boundary layer growth in a changing climate.” *Geophysical Research Letters* 41(4): 1290–1294, <https://doi.org/10.1002/2013GL058826>
- Eyring, V, S Bony, GA Meehl, CA Senior, B Stevens, RJ Stouffer, and KE Taylor. 2016. “Overview of the Coupled Model Intercomparison Project Phase 6 (CMIP6) experimental design and organization.” *Geoscientific Model Development* 9(5): 1937–1958, <https://doi.org/10.5194/gmd-9-1937-2016>
- Santanello, JA, PA Dirmeyer, CR Ferguson, KL Findell, AB Tawfik, A Berg, M Ek, P Gentine, BP Guillod, C van Heerwaarden, J Roundy, and V Wulfmeyer. 2018. “Land-Atmosphere Interactions: The LoCo Perspective.” *Bulletin of the American Meteorological Society* 99(6): 1253–1272, <https://doi.org/10.1175/BAMS-D-17-0001.1>
- Schiro, KA, JD Neelin, DK Adams, and BR Lintner. 2016. “Deep convection and column water vapor over tropical land versus tropical ocean: A comparison between the Amazon and the tropical western Pacific.” *Journal of the Atmospheric Sciences* 73(10): 4043–4063, <https://doi.org/10.1175/JAS-D-16-0119.1>
- Su, T, and Z Li. 2023. “Planetary Boundary Layer Height (PBLH) over SGP from 1998 to 2023.” U.S. Department of Energy, Atmospheric Radiation Measurement user facility, Richland, Washington. Data set. <https://doi.org/10.5439/2007149>
- Su, T, Y Zheng, and Z Li. 2022. “Methodology to determine the coupling of continental clouds with surface and boundary layer height under cloudy conditions from lidar and meteorological data.” *Atmospheric Chemistry and Physics* 22(2): 1453–1466, <https://doi.org/10.5194/acp-22-1453-2022>
- Su, T, Z Li, and R Kahn. 2020. “A new method to retrieve the diurnal variability of planetary boundary layer height from lidar under different thermodynamic stability conditions.” *Remote Sensing of Environment* 237: 111519, <https://doi.org/10.1016/j.rse.2019.111519>
- Taylor, KE. 2001. “Summarizing multiple aspects of model performance in a single diagram”. *Journal of Geophysical Research – Atmospheres* 106(D7): 7183–7192, <https://doi.org/10.1029/2000JD900719>
- Taylor, KE, RJ Stoufer, and GA Meehl. 2012. “An overview of CMIP5 and the experiment design.” *Bulletin of the American Meteorological Society* 93(4): 485–498, <https://doi.org/10.1175/BAMS-D-11-00094.1>
- Tang, S, C Tao, S Xie, and M Zhang. 2019. Description of the ARM Large-Scale Forcing Data from the Constrained Variational Analysis (VARANAL) – Version 2. U.S. Department of Energy, Atmospheric Radiation Measurement user facility, Richland, Washington. DOE/SC-ARM-TR-222. <https://doi.org/10.5439/1273323>

Xie, SC, RT Cederwall, and MH Zhang. 2004. “Developing long-term single-column model/cloud system-resolving model forcing data using numerical weather prediction products constrained by surface and top of the atmosphere observations.” *Journal of Geophysical Research – Atmospheres* 109(D1): D01104, <https://doi.org/10.1029/2003jd004045>

Xie, S, RB McCoy, SA Klein, RT Cederwall, WJ Wiscombe, EE Clothiaux, KL Gaustad, JC Golaz, SD Hall, MP Jensen, KL Johnson, Y Lin, CN Long, JH Mather, RA McCord, SA McFarlane, G Palanisamy, Y Shi, and DD Turner. 2010. “ARM Climate Modeling Best Estimate Data: A New Data Product for Climate Studies.” *Bulletin of the American Meteorological Society* 91(1): 13–20, <https://doi.org/10.1175/2009bams2891.1>

Zhang, C, S Xie, SA Klein, H-Y Ma, S Tang, K Van Weverberg, CJ Morcrette, and J Petch. 2018. “CAUSES: Diagnosis of the summertime warm bias in CMIP5 climate models at the ARM Southern Great Plains site.” *Journal of Geophysical Research – Atmospheres* 123(6): 2968–2992, <https://doi.org/10.1002/2017JD027200>

Zhang, C, S Xie, C Tao, S Tang, T Emmenegger, JD Neelin, KA Schiro, W Lin, and Z Shaheen. 2020. “The ARM Data-Oriented Metrics and Diagnostics Package for Climate Models – A New Tool for Evaluating Climate Models with Field Data.” *Bulletin of the American Meteorological Society* 101(10): E1619–E1627, <https://doi.org/10.1175/BAMS-D-19-0282.1>

Zhang, M, and J Lin. 1997. “Constrained variational analysis of sounding data based on column-integrated budgets of mass, heat, moisture, and momentum: Approach and application to ARM measurements.” *Journal of the Atmospheric Sciences* 54(11): 1503–1524, [https://doi.org/10.1175/1520-0469\(1997\)054<1503:CVAOSD>2.0.CO;2](https://doi.org/10.1175/1520-0469(1997)054<1503:CVAOSD>2.0.CO;2)

Zhang, MH, JL Lin, RT Cederwall, JJ Yio, and SC Xie. 2001. “Objective analysis of ARM IOP data: Method and sensitivity.” *Monthly Weather Review* 129(2): 295–311, [https://doi.org/10.1175/1520-0493\(2001\)129<0295:oaoid>2.0.co;2](https://doi.org/10.1175/1520-0493(2001)129<0295:oaoid>2.0.co;2)

Zheng, X, B Xi, X Dong, T Logan, Y Wang, and P Wu. 2020. “Investigation of aerosol–cloud interactions under different absorptive aerosol regimes using Atmospheric Radiation Measurement (ARM) southern Great Plains (SGP) ground-based measurements.” *Atmospheric Chemistry and Physics* 20(6): 3483–3501, <https://doi.org/10.5194/acp-20-3483-2020>

Zheng, X, C Tao, C Zhang, S Xie, Y Zhang, B Xi, and X Dong. 2023. “Assessment of CMIP5 and CMIP6 AMIP Simulated Clouds and Surface Shortwave Radiation Using ARM Observations over Different Climate Regions.” *Journal of Climate* 36(24): 8475–8495, <https://doi.org/10.1175/JCLI-D-23-0247.1>



www.arm.gov

U.S. DEPARTMENT OF
ENERGY

Office of Science